BJR

■ **FOOT & ANKLE**

Tibial cortex transverse transport accelerates wound healing via enhanced angiogenesis and immunomodulation

Y. Yang,
Y. Li,
Q. Pan,
S. Bai,
H. Wang,
X. Pan,
K-K. Ling,
G. Li

From The Chinese University of Hong Kong, Prince of Wales Hospital, Hong Kong, China

Aims

Treatment for delayed wound healing resulting from peripheral vascular diseases and diabetic foot ulcers remains a challenge. A novel surgical technique named 'tibial cortex transverse transport' (TTT) has been developed for treating peripheral ischaemia, with encouraging clinical effects. However, its underlying mechanisms remain unclear. In the present study, we explored the potential biological mechanisms of TTT surgery using various techniques in a rat TTT animal model.

Methods

A novel rat model of TTT was established with a designed external fixator, and effects on wound healing were investigated. Laser speckle perfusion imaging, vessel perfusion, histology, and immunohistochemistry were used to evaluate the wound healing processes.

Results

Gross and histological examinations showed that TTT technique accelerated wound closure and enhanced the quality of the newly formed skin tissues. In the TTT group, haematoxylin and eosin (H&E) staining demonstrated a better epidermis and dermis recovery, while immunohistochemical staining showed that TTT technique promoted local collagen deposition. The TTT technique also benefited to angiogenesis and immunomodulation. In the TTT group, blood flow in the wound area was higher than that of other groups according to laser speckle imaging with more blood vessels observed. Enhanced neovascularization was seen in the TTT group with double immune-labelling of CD31 and α-Smooth Muscle Actin (α-SMA). The number of M2 macrophages at the wound site in the TTT group was also increased.

Conclusion

The TTT technique accelerated wound healing through enhanced angiogenesis and immunomodulation.

Article focus

■ To establish a reproducible animal model of tibial cortex transverse transport (TTT) with standardized surgical protocols to mimic its clinical application.

■ To verify the therapeutic effects of TTT on skin wound defect healing in the established rat model.

■ To explore the underlying biological mechanisms of TTT promoting wound healing with a focus on angiogenesis and immunomodulation.

Key messages

■ Using a specially designed external fixator, we successfully established a standardized rat model of TTT which mimics the clinical procedure.

■ TTT promotes wound healing via its regulating effects on angiogenesis and immunomodulation, and may be an alternative treatment option for chronic ischaemic conditions.

Correspondence should be sent to Gang Li; email:
gangli@cuhk.edu.hk

Strengths and limitations

■ Using a customized external fixator and standard surgical procedures, we established a novel rat model of TTT, which can be used for studying the biological mechanisms of TTT in depth.

■ We confirmed that TTT surgery could effectively promote wound healing through radiological, histological, and immunohistochemical examinations in the rat model.

■ In clinical research, the effects of TTT surgery on lower limb ischaemic diseases have been promising in recent years, however the underlying mechanisms are still lacking. In the present study, we confirmed that TTT surgery promoted wound healing via its regulating effects on angiogenesis and immunomodulation, providing more biological mechanisms for its clinical applications in the management of chronic ischaemic diseases.

■ Sprague-Dawley (SD) rats with acute wound defect were used, which could not entirely mimic the clinical conditions such as chronic wounds or diabetic ulcers.

■ The findings from animal studies may not directly apply to humans.

Introduction

Chronic limb ischaemic diseases frequently involve peripheral vascular impairments and occlusion, leading to severe ulcers which are difficult to manage via both conservative and/or surgical treatments.[1] These chronic non-healing conditions may eventually lead to a high incidence of amputation.[2] To explore efficient management of chronic limb ischaemic diseases, the Ilizarov bone-lengthening technique has been considered for its promising effects on neovascularization and tissue regeneration.[3-5] The Ilizarov technique has been widely used for the management of fracture nonunions, limb discrepancy, severe deformities, and bone defects, also known as the distraction osteogenesis (DO) technique, which is a process from mechanotransduction to osteogenesis.[6-9] During the DO treatment, a rich vascular network formation is found in the newly formed bone and surrounding soft-tissues, which is responsible for rapid tissue formation and remodelling, leading to the development of the new concept termed distraction histogenesis (DH).[10] Governed by the tension-stress rule of tissue regeneration, the DH technique promotes tissue regeneration by regulation of signalling transduction molecules and inflammatory, angiogenic, and epigenetic factors that control gene expression.[11] DH could awaken the body's innate self-regeneration potentials and has been adopted in the development of novel treatment strategies for many challenging diseases.

Transverse bone transport surgery was first described briefly by Ilizarov in 1989 for the management of soft-tissue healing.[6] Qu et al[12] reported the use of tibial cortex transverse transport (TTT) surgery for the successful management of thromboangitis obliterans in 2001. Hua et al[13] reported the use of TTT surgery for the management of severe diabetic foot ulcers in 2020. Despite the successful clinical applications of TTT surgery, mechanistic studies are still lacking. To perform TTT surgery in small animals is surgically challenging, and there is an urgent need to develop a proper animal model to study the mechanisms of TTT surgery.

The current study reported a rat model of TTT surgery. The rat TTT surgery model was established with standard instrumentation and surgical procedures to ensure its reproducibility, and the model was used to explore the mechanisms of TTT surgery on foot wound healing.

Methods

Instrumentation for rat TTT surgery. To simulate the clinical procedure of TTT surgery in a rat model, a specially designed external fixator device was manufactured. Modified from the clinically available external fixator for TTT surgery (BFIX, Transverse Bone Transport System, China Patent 201610722035.5; CE Marking 0197; Aike Shanghai Medical Instrument Co. Ltd., China),[14,15] we redesigned the fixator by reducing the size to fit on rat tibia. As shown in Figure 1a, the external fixator is composed of four parts: 1) two 20 mm long screws (1 mm in diameter) for fixing the fixator on the tibia; 2) two 10 mm long small screws (0.8 mm in diameter) for fixing the cortical bone chip; 3) a turning nut for moving the cortical bone chip inward or outward from the tibial shaft; and 4) the external fixator frame.

Study design. All experiments were approved by the Animal Research Ethics Committee of The Chinese University of Hong Kong (AEEC number: 20 - 095-ECS). We have included an ARRIVE checklist to show that we have conformed to the ARRIVE guidelines. A total of 36 Sprague-Dawley rats (13-week-old, male, mean weight of 280 g (standard deviation (SD) 13.4)) were used in this study. The sample size was calculated based on our pilot study, where we compared the wound healing rate with or without TTT treatment. Using power calculation with a probability of 90%, we estimated the sample size as six rats per group per analysis (Supplementary Figure a). All rats were randomized into three groups, with 12 rats per group: sham group (negative control); fixator group (positive control); and TTT group. In sham group, rats were given a sham surgery without fixator implanted and served as negative control, whereas rats in fixator and TTT groups received TTT fixator implantation surgery. Full-thickness skin defects were created on the right foot dorsal side on all rats during the surgery. Bone chip transportation was performed on rats in TTT group. No infection or other complications of rats were observed after the surgery. All rats were included for data analysis. To minimize potential confounders, all animals in TTT group received bone transverse transporting simultaneously, and analyses were done blindly by two independent
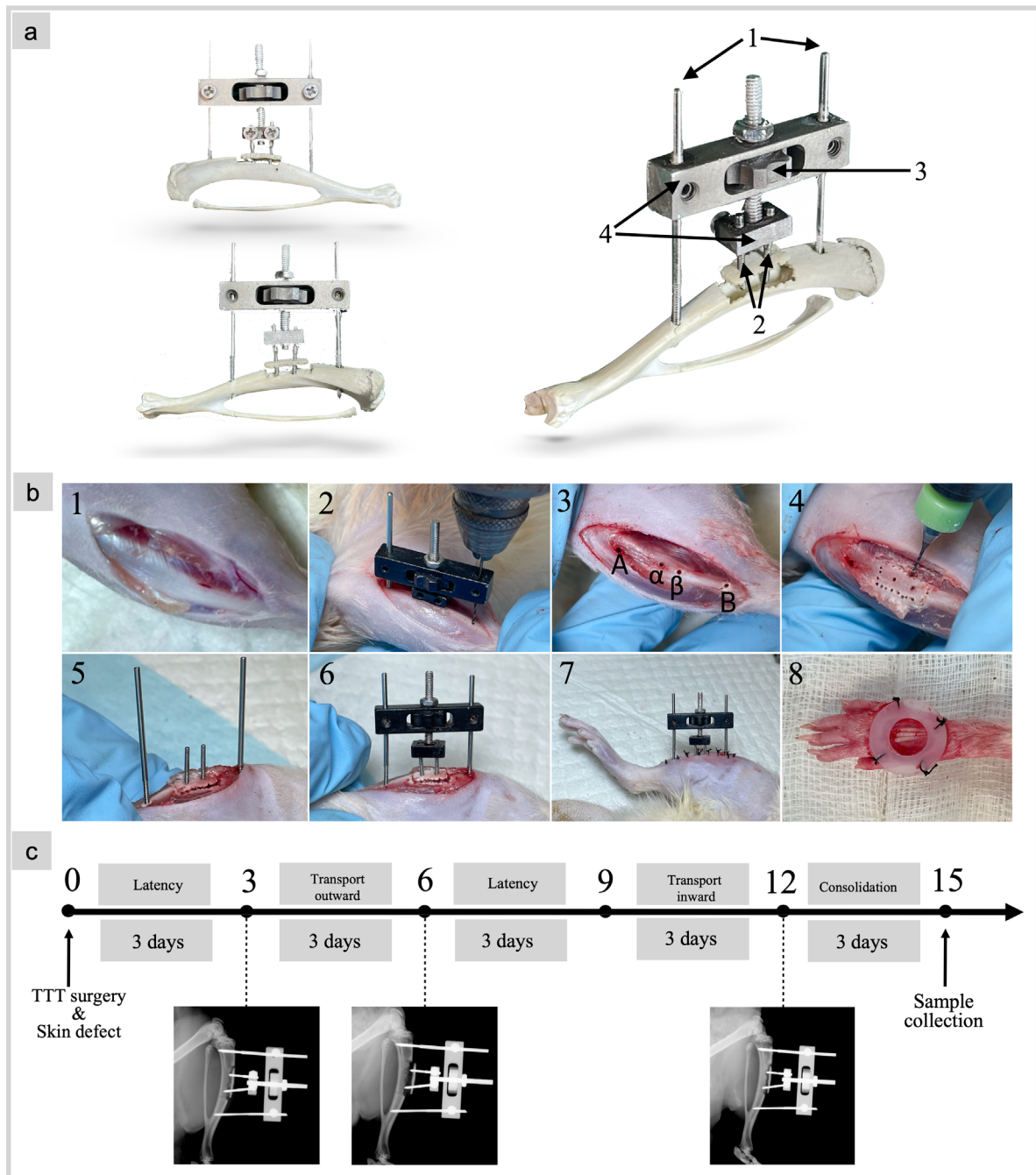
Fig. 1

Introduction of tibial cortex transverse transport (TTT) external fixator, surgical procedure and workflow. a) Components of TTT external fixator: 1) two long screws; 2) two small screws; 3) a turning nut; and 4) the external fixator frame. b) Surgical procedure of TTT technique and skin defect: 1) The right tibia was exposed; 2) and 3) guided with the external fixator, holes A, B, α, and β were drilled; 4) pinholes were drilled around holes α and β, forming a bone window; 5) four screws were inserted; 6) and 7) the cortical bone chip was dislocated, and the external fixator was assembled and incision sutured; and 8) a silicone splint was fixed to the wound skin. c) Workflow of TTT application. A radiograph was taken to track the cortical bone chip status.

researchers (SB, HW). Group allocation and randomization was performed by the third independent researcher (QP).

Surgical procedure for rat TTT surgery. The surgical protocol for animal surgery was modified from our clinical protocol for minimal invasive TTT surgery.[14] In brief, anaesthesia was maintained by intraperitoneal injection of ketamine (75 mg/kg) and xylazine (10 mg/kg) in phosphate-buffered saline (PBS), and the right tibia was exposed with a 3 cm long incision via an anterior approach (Figure 1b (part 1)). Guided with the external fixator, two 0.8 mm transosseous holes (holes A and B) for the proximal and distal fixator screws and two 0.5 mm cortex penetrating holes (holes α and β) for cortical graft fixation
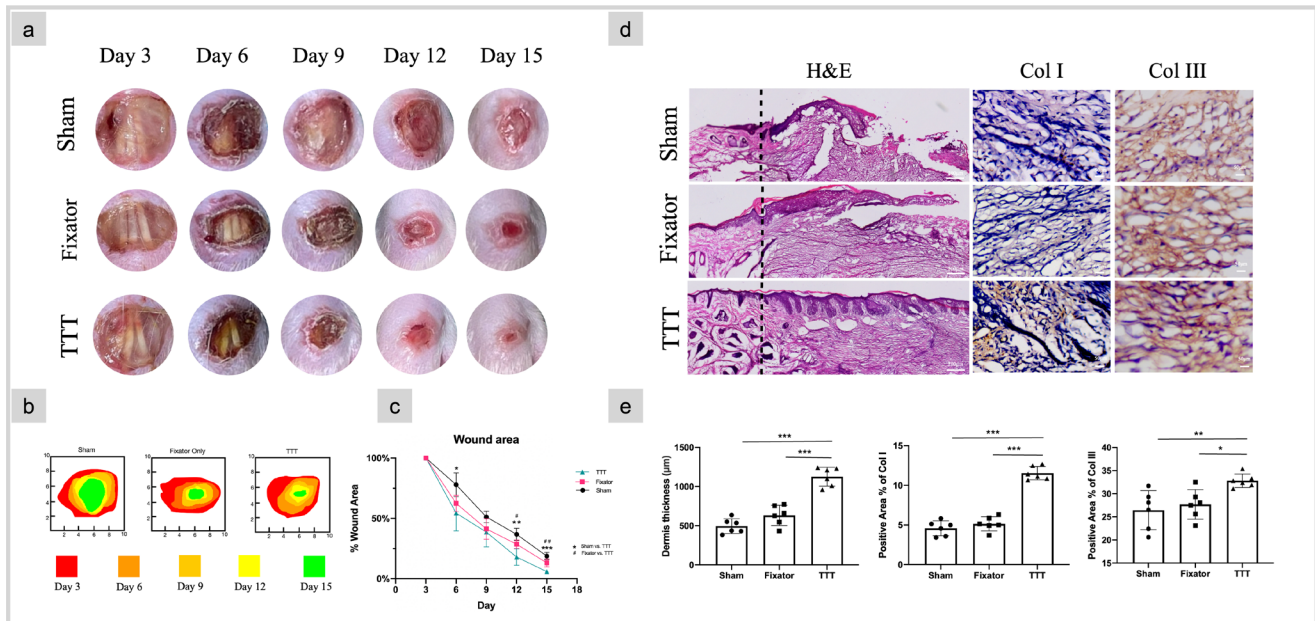
Fig. 2

Tibial cortex transverse transport (TTT) technique promoted skin tissue recovery. a) Representative images of wound healing progress for three groups from the same Sprague-Dawley rat. b) Traces of wound-bed closure during 15 days. c) Wound area for each group during 15 days. d) In haematoxylin and eosin (H&E) staining, better continuous epidermis was observed in the TTT group. Scale bar 100 μm, 100× magnification. In immunohistochemical staining of Anti-Collagen I antibody and Anti-Collagen III antibody (IHC-Col I&III), the extracellular matrix shows tighter fibre arrangement and collagen deposition in the TTT group. Scale bar 50 μm, 200× magnification. e) Semi-quantitative analysis showed thicker dermis in the TTT group (TTT vs Fixator, p < 0.001; TTT vs Sham, p < 0.001, Tukey's multiple comparison test). Positive areas of collagen types I and III deposition were both larger than that of the other two groups (for Col I, TTT vs Fixator, p < 0.001, TTT vs Sham, p < 0.001; for Col III, TTT vs Fixator, p = 0.034, TTT vs Sham, p = 0.009; Tukey's multiple comparison test) Graphics were generated by Leica Application Suite, Leica Camera AG, Germany. Data were measured as means (standard deviations), *p < 0.05, **p < 0.01, ***p < 0.001, n = 6.

were drilled (Figure 1b (parts 2 to 3)). The proximal transosseous hole (hole A) was 5 mm under the tibial plateau. To perform the corticotomy, a series of pinholes were firstly drilled around holes α and β, forming a 5 × 10 mm rectangular bone window on the tibial shaft (Figure 1b (part 4)). The two 1 mm and two 0.8 mm screws were then inserted (Figure 1b (part 5)). Then the cortical bone chip was carefully dislocated from tibial shaft by joining the holes together using a sharp knife. The external fixator was assembled, and the incision was sutured (Figure 1b (parts 6 and 7)). Radiographs were taken periodically to confirm the cortical bone chip movement back/forth on the tibial shaft (Figure 1c).

Skin defect model. A full-thickness skin defect with a diameter of 4 mm was created using a sharp circular cutter on the right foot dorsal side following the successful TTT surgery. A donut-shaped silicone splint (8 mm inner diameter, 2 mm thickness) was placed around the perimeter of the wound and fixed to the wound edge skins by 5-0 silk sutures (Figure 1b (part 8)).

Cortical bone chip transport. Cortical bone chip transport was performed by turning the nut on the external fixator. After a three-day postoperative latency, the bone chip was transversely pulled outward with 0.25 mm every 12 hours for three days, making the total transport distance of 1.5 mm. After maintaining this position for three days, the bone chip was pushed inward at the same speed of 0.25 mm every 12 hours for three days. Radiographs were used to confirm the position of the bone chip back to the original place at the tibial shaft (Figure 1c). The procedure for TTT treatment was nine days.

Observation of skin wound healing. The general healing condition of the skin defect (n = 6) was macroscopically monitored and recorded by digital photography on day 0, 3, 6, 9, 12, and 15 after the skin defect surgery. The wound boundaries were traced and wound area was measured by ImageJ software (National Institutes of Health, USA) according to previously described methods.[16] Wound area% was calculated by normalizing wound area with the original (day 0) wound area.

Laser speckle perfusion imaging. Under anaesthesia with isoflurane, the blood flow of the wound area was visualized with a laser speckle imaging system (RWD Life Science, China) on day 3, 6, 9, 12, and 15 following the defect surgery (n = 6). The foot was fixed on the examination pad and placed 15 cm below the detector. The focus was adjusted to achieve a clear blood flow image, and all photos were taken under the same zoom (1×), exposure time (5 ms), and pseudo-colour threshold (228 to 250) settings. The original defect area and the same area on the contralateral foot were selected as the region of interest (ROI). The blood flow rate of the wound area
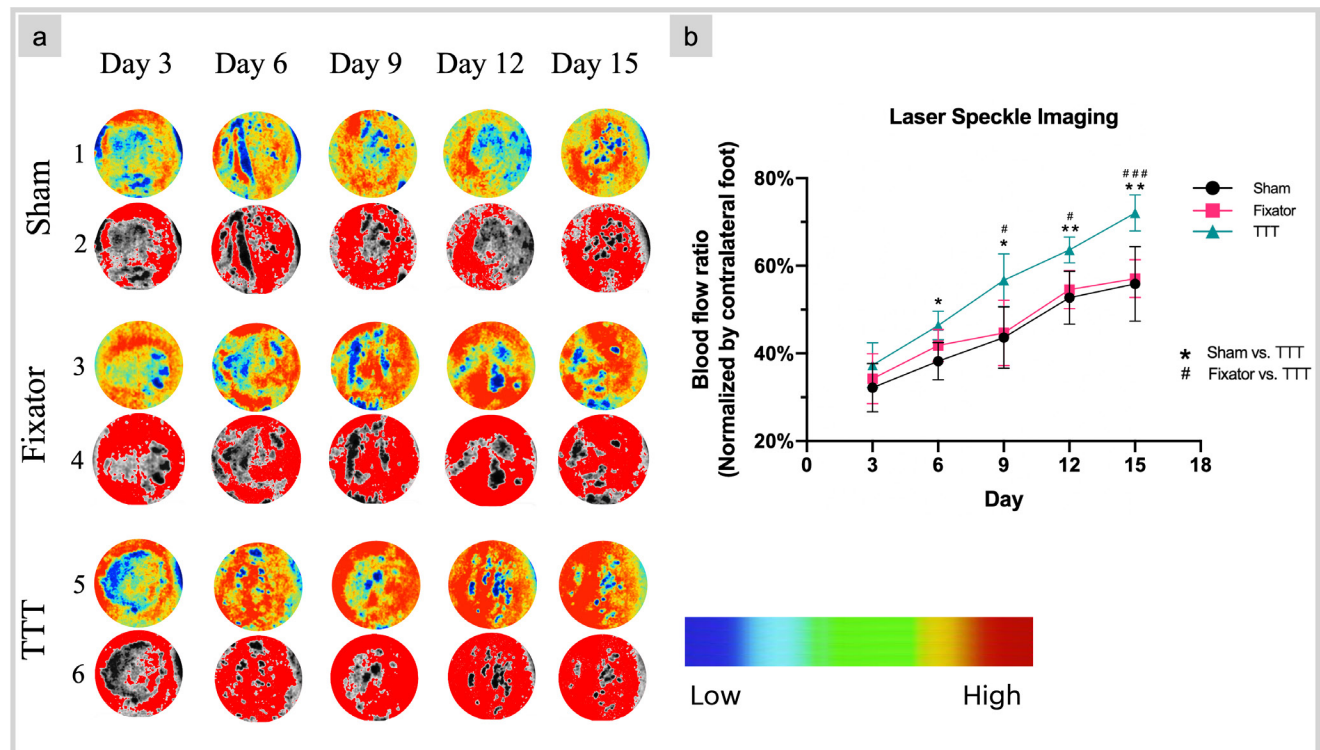
Fig. 3

Tibial cortex transverse transport (TTT) technique elevated local blood flow. a) The images of rows 1, 3, and 5 are blood flow changes around the wound, recorded by Laser Speckle perfusion imaging (1.2× magnification) every three days. The images of rows 2, 4, and 6 are corresponding red channel for areas measured by ImageJ (USA). The colour bar represents blood flow (or perfusion) levels, from blue (low) to red (high). b) The TTT group showed the best blood perfusion among the three groups, especially in the last three days (on day 12, TTT vs Fixator, $p = 0.006$, TTT vs Sham, $p = 0.013$; on day 15, TTT vs Fixator, $p < 0.001$, TTT vs Sham, $p = 0.009$; Tukey's multiple comparison test). Data were measured as means (standard deviations), $*p < 0.05$, $**p < 0.01$, $\#p < 0.05$, $\#\#\#p < 0.001$, $n = 6$.

at different time points was measured by the built-in software (Application Revision: V 01.00.00.6642; BORD Revision: V01.00.00) and normalized with the contralateral side.

Blood vessel perfusion and micro-CT scanning. Six rats from each group were terminated 15 days following skin defect surgery. At the time of termination, blood vessel perfusion was performed using our established protocol.[17] Briefly, under general anaesthesia, rats underwent laparotomy to expose the abdominal aorta. The upper segment of the aorta was ligated, and arterial puncture was made below the ligation using a 23 G butterfly needle. After flushing completely with heparinized normal saline (1,000 U/ml) at a constant pressure of approximately 150 mmHg, vasculature was then pressure-fixed with formalin, euthanasia ensured, and followed by perfusion of Microfil MV-117 (Flow Tech, USA). Adequate perfusion was determined and verified by gross examination of the feet and toes, for an apparent orange colour change similar to that of Microfil. Samples were kept at 4°C for 24 hours for complete solidification. The full-thickness skin samples within the wound area were collected and subjected to micro-CT (μCT) scanning using a high-resolution μCT (μCT40 Scanco Medical, Switzerland).

The original skin defect areas were selected as the ROI. Vessel volumes were recorded for data analysis.

Histology and immunohistochemistry staining. Six rats from each group were terminated 15 days following skin defect surgery. The samples containing the entire skin defect areas were collected, fixed in 10% formalin for 24 hours at room temperature, and then subject to cryosection after embedding with optimal cutting temperature compound (O.C.T., SAKURA Tissue-Tek, Japan). Then 5 μm sections were cut using a rotary microtome (HM 355 S, Thermo Fisher Scientific, Germany) along the long axis of tibia in the sagittal plane. Haematoxylin and eosin (H&E) staining, immunohistochemistry, and immunofluorescence staining were performed. Immunohistochemistry and immunofluorescence staining were performed using standard protocols as reported in an earlier study.[17] The following antibodies were used: rabbit anti-rat anti-Collagen I antibody (Col I, Abcam, UK; ab34710, 1:100); rabbit anti-rat Col III (Col III, Abcam; ab7778, 1:100); goat anti-rat CD31 (R & D Systems, USA; 10 ug/ml, AF3628); mouse anti-α-SMA (α-SMA, Abcam; ab7817, 1:100); rabbit anti-rat Anti-inducible nitric oxide synthase antibody (iNOS, Abcam; ab15323, 1:150); and rabbit anti-rat CD206 (CD206, Abcam; ab64693, 1:100).
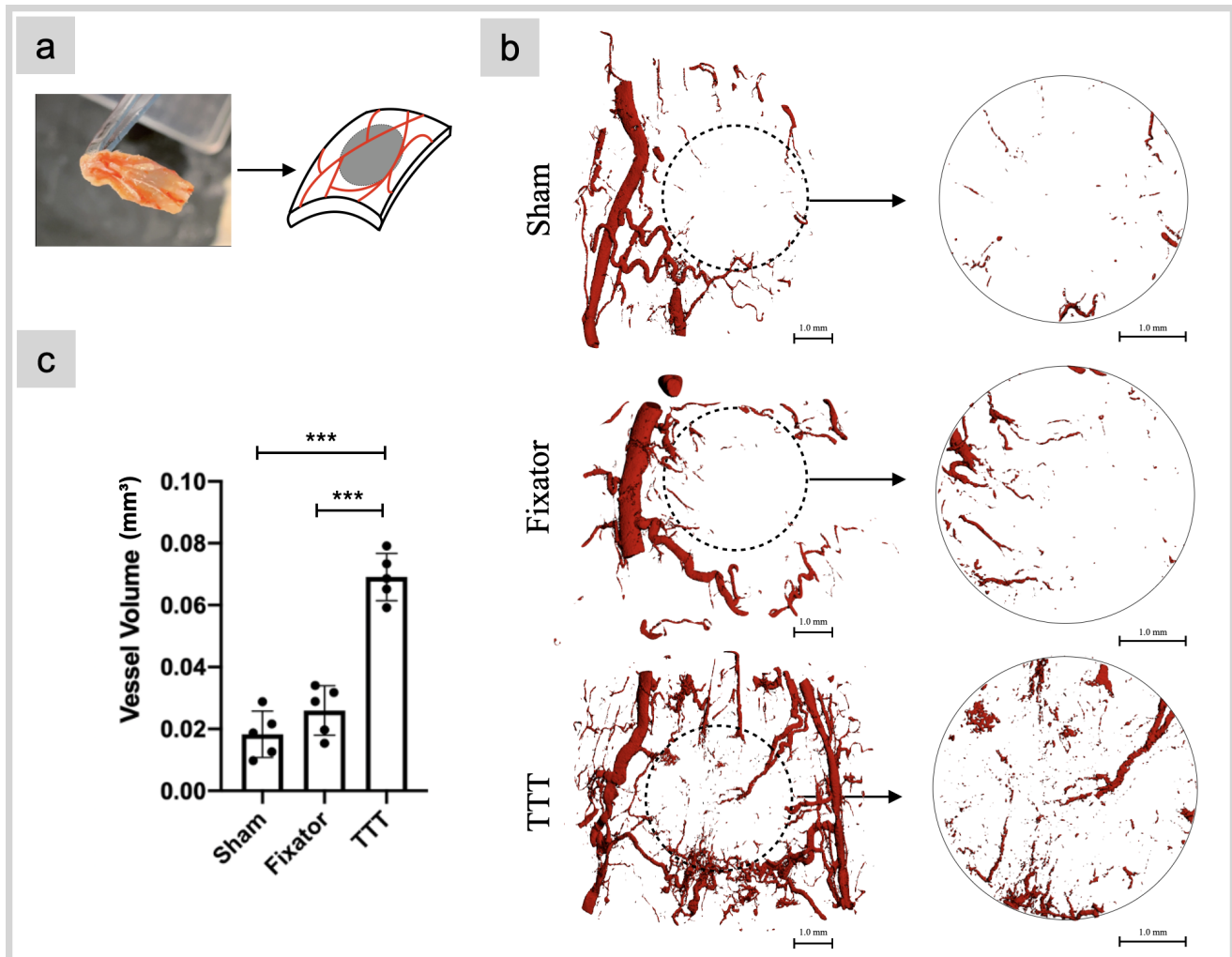
Fig. 4

Tibial cortex transverse transport (TTT) technique enhanced angiogenesis. a) Illustration of sample collection. The collected skin was scanned using micro-CT (μCT), while the grey round area is the region of interest (ROI) for semi-quantitative analysis. b) To perform vessel volume analysis, the ROI images in the right column were selected from the dash line circle of the left column. Results showed that more blood vessels were formed inside the newly formed skins in the TTT group. c) Quantitative analysis showed that the vessel volume in the wound area in the TTT group was significantly higher than that of the control and fixator groups (TTT vs Fixator, p < 0.001, TTT vs Sham, p < 0.001, Tukey's multiple comparison test). Data were measured as means (standard deviations), ***p < 0.001, n = 6.

Semi-quantitative analysis of respective staining was performed using ImageJ as previously reported.[17]

Statistical analysis. All quantitative data were analyzed using SPSS v18.0 software for Windows (SPSS, USA). One-way analysis of variance (ANOVA), Skewness and Kurtosis, and Tukey's multiple comparison test were used to confirm the data normal distribution and to compare the mean values. Statistical significance was set at p < 0.05.

Results

TTT accelerated the wound closure. The wound area (n = 6) calculated with ImageJ software from day 6 to day 15 significantly reduced in the TTT group compared to the untreated group (Figures 2a to 2c). The highest wound closure rate was achieved in the TTT group, followed by the fixator group (Figures 2a and 2b). On days 12 and 15, the area of unhealed wound in the TTT group was smaller than that of the untreated control and fixator groups with a significant difference (on day 12, TTT vs Fixator, p = 0.025, TTT vs Sham, p = 0.001; on day 15, TTT vs Fixator, p = 0.004, TTT vs Sham, p < 0.001; Tukey's multiple comparison test) (Figure 2c), indicating that wound closure was accelerated by the TTT treatment.

TTT improved the quality of newly healed skin tissues. On day 15, histology (n = 6) showed that the newly formed epidermis at the wound site was discontinuous, and uneven in the control and fixator groups, whereas continuous epidermis with epithelial lining was clearly seen in the TTT group (Figure 2d). The mean thickness of the newly formed dermis in the TTT group was significantly higher than that in the other groups (TTT vs Fixator, p
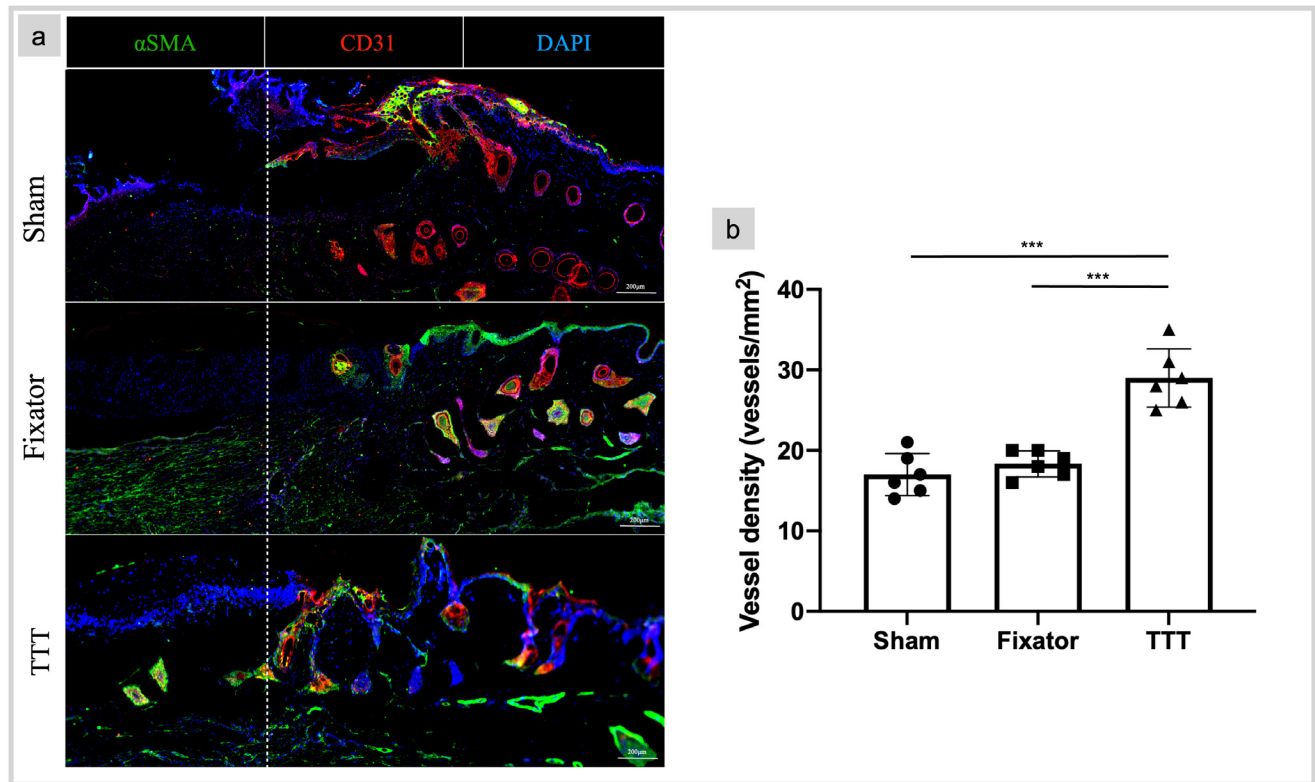
Fig. 5

Tibial cortex transverse transport (TTT) technique enhanced small vessels in the newly formed skins. a) Wound sections were double-labelled for CD31 (red) and α-SMA (green). Nuclei were stained with 4',6-Diamidino-2-Phenylindole (DAPI, blue). Large vessels were mainly located near the edge of healthy skin, and smaller vessels were seen inside the newly formed dermis. b) Semi-quantitative measurement of immunostaining showed that the amount of blood vessels in the TTT group was significantly higher than that of the other groups (TTT vs Fixator, $p < 0.001$, TTT vs Sham, $p < 0.001$; Tukey's multiple comparison test). Graphics were generated by Leica Application Suite. Data were measured as means (standard deviations), ***$p < 0.001$, n = 6.

< 0.001; TTT vs Sham, $p < 0.001$, Tukey's multiple comparison test) (Figure 2e). The collagen deposition in the wound area was checked by immunostaining of type I and III collagen, and the collagen fibres in the wound areas of the TTT group were tightly and neatly orientated; in contrast, parse and disordered collagen fibres were seen in the wound areas of the control group. Semi-quantitative analysis showed that the TTT group had the highest positive staining areas for both Col I and Col III among all three groups, followed by the fixator group, with a significant difference (for Col I, TTT vs Fixator, $p < 0.001$, TTT vs Sham, $p < 0.001$; for Col III, TTT vs Fixator, $p = 0.034$, TTT vs Sham, $p = 0.009$; Tukey's multiple comparison test) (Figure 2e).

TTT promoted angiogenesis in wound healing. During the cortical bone transport, changes in blood flow at the wound area (n = 6) were recorded using Laser Speckle perfusion imaging every three days. From day 6 to day 15, the blood flow in the wound area was significantly elevated in the TTT group compared to the fixator and control groups (Figure 3). Angiography after blood vessel perfusion was performed to exam the blood vessel distribution in the wound area on day 15, and showed that more blood vessels were formed inside the newly formed skins in the TTT group (Figure 4b). Quantitative analysis showed that the vessel volume in the wound area in the TTT group was significantly higher than that of the control and fixator groups (Figure 4c).

Immunofluorescence staining with double labelling of CD31 and α-SMA was carried out to determine the blood vessels in the newly formed skins. In all three groups, large vessels were mainly located near the edge of healthy skin, and smaller vessels were seen inside the newly formed dermis. Semi-quantitative measurement of immunostaining showed that the amount of blood vessels in the TTT group was significantly higher than that of the other groups (TTT vs Fixator, $p < 0.001$, TTT vs Sham, $p < 0.001$; Tukey's multiple comparison test) (Figure 5).

TTT regulated the local inflammatory responses through modulating M1 and M2 macrophages. Immunostaining of iNOS and CD206 was used to identify M1 and M2 macrophages within the wound areas (n = 6). As shown in Figure 6a, in the TTT group at day 15, the population of M1 macrophages was significantly reduced (Figure 6b) and M2 macrophages were significantly increased (Figure 6c) with statistical significance compared to the sham and
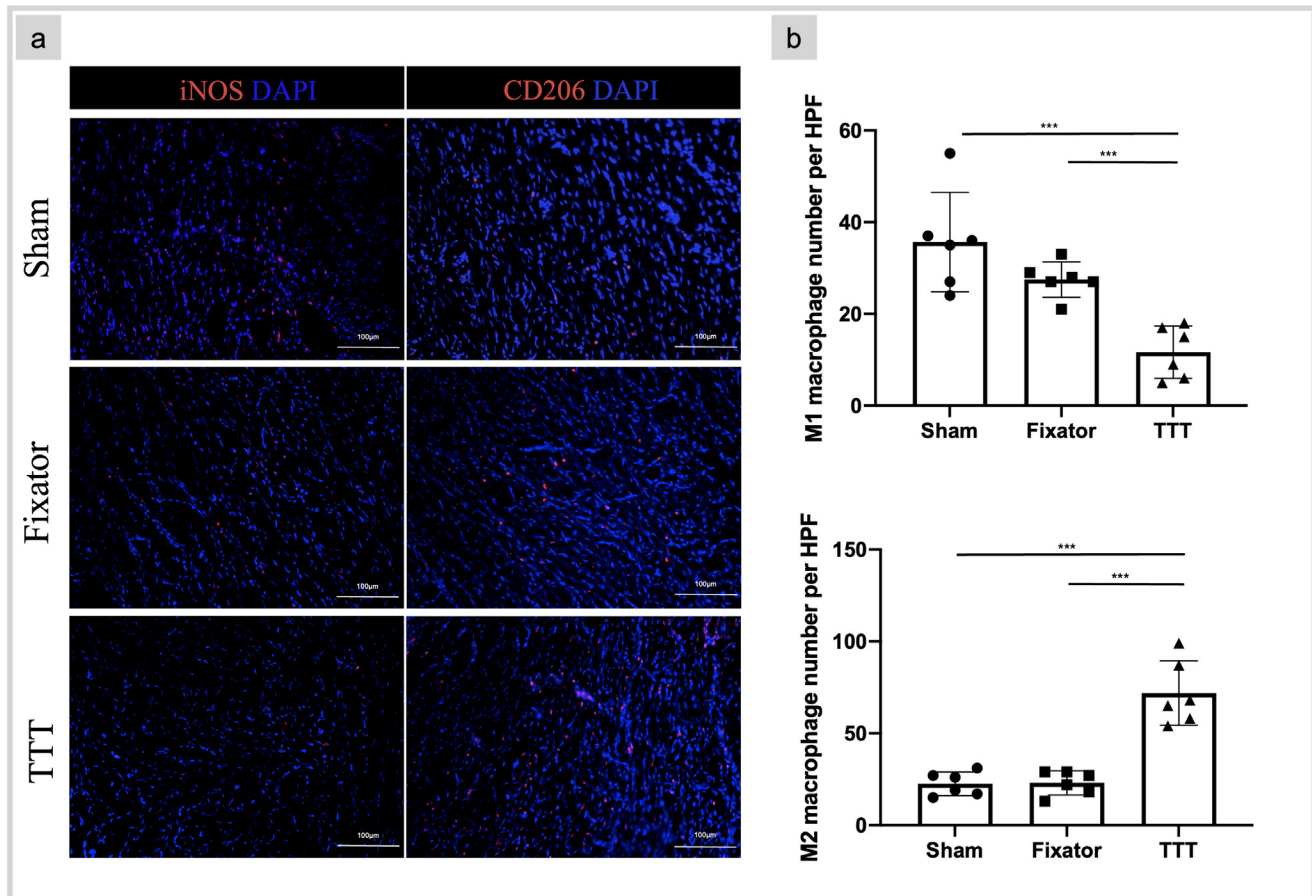
Fig. 6

Tibial cortex transverse transport (TTT) technique regulated the local inflammatory responses through M1 and M2 macrophages. a) Representative images of immunofluorescence staining of inducible nitric oxide synthase antibody (iNOS) (red) for M1 and Mannose (red) for M2 from wound skin on day 15. Fewer M1 macrophages were observed in the TTT group. Significantly larger numbers of M2 were seen in the TTT group compared to the sham and fixator groups. b) Semi-quantitative measurement of population of M1 macrophages was significantly reduced and M2 macrophages were significantly increased (for M1, TTT vs Fixator, $p = 0.006$, TTT vs Sham, $p < 0.001$; for M2, TTT vs Fixator, $p < 0.001$, TTT vs Sham, $p < 0.001$; Tukey's multiple comparison test). Graphics were generated by Leica Application Suite (LAS). Data were measured as means (standard deviations), ***$p < 0.001$, $n = 6$. DAPI, 4',6-Diamidino-2-Phenylindole; HPF, high power field.

fixator groups (for M1, TTT vs Fixator, $p = 0.006$, TTT vs Sham, $p < 0.001$; for M2, TTT vs Fixator, $p < 0.001$, TTT vs Sham, $p < 0.001$; Tukey's multiple comparison test).

Discussion

TTT surgery is an emerging new surgical procedure for the management of severe chronic limb ischaemic diseases such as diabetic foot ulcers. The pathophysiology of diabetic foot ulcers has neuropathic, vascular, and immune system components, which are all related to the hyperglycaemic state of diabetes.[18,19] Hyperglycaemia produces oxidative stress on nerve cells and leads to neuropathy.[19] Additional nerve dysfunction follows from glycosylation of nerve cell proteins, leading to further ischaemia. Vascular changes that lead to diabetic foot ulcers correlate with hyperglycaemia-induced changes in the peripheral arteries of the foot.[19] Endothelial cell dysfunction leads to a decrease in vasodilators and increase in plasma thromboxane A2 levels.[20] Vasocontraction and plasma hypercoagulation in peripheral arteries

lead to increased risks of ischaemia and ulceration. In addition, immune function changes such as reduced healing response and increased T lymphocyte apoptosis have been found in diabetic foot ulcer patients.[20]

The lack of a TTT animal model hinders its mechanistic studies. The current study reported the establishment of a rat TTT animal model which replicates the clinical procedure of TTT surgery. Furthermore, we confirmed the therapeutic benefits of TTT on wound healing in this model and investigated the possible biological mechanisms.

A recent clinical study reported that TTT surgery ameliorated vascular insufficiency and promoted wound healing by promoting microcirculation in the ischaemic limbs.[21] Besides, an expert consensus has been published in 2020 with clear recommendations for indications, contraindications, principles for surgical procedures, and preoperative and postoperative managements, to maximize the success rate of TTT surgery in the treatment of severe diabetic foot ulcer.[13] The current study demonstrated that after TTT treatment, angiogenesis was

significantly promoted. Neovascularization and increased blood perfusion were found following TTT treatment, in agreement with the clinical observations.[13,21] It is well known that a vigorous and dynamic angiogenic response is a prerequisite for successful healing of connective tissues.[22,23] During wound healing, the demand for oxygen and nutrients is high due to robust capillary growth, cellular proliferation, migration, and metabolic activities.[24] At the proliferation phase of wound healing, we observed enhanced angiogenesis following TTT treatment, in that increased endothelial progenitor cells (EPCs) (CD31/α-SMA positive cells) were evident in the wound areas, confirming that TTT promotes angiogenesis.

Immunomodulatory responses were also observed after TTT treatment. Macrophages M1 and M2 are important during the inflammation and proliferation phase of tissue repair.[25,26] The first three to five days following skin injury is the haemostasis and inflammation phase of healing when M1 macrophages are the most prominent cells, which are first recruited to clean up the senescent cells and debris within the wound.[27,28] The wound closure progress and blood flow did not differ among the three groups in the first nine days in the current study, indicating that TTT may mainly affect the late stage of healing. For example, during the proliferation phase of cutaneous wound healing, TTT significantly promoted M1 macrophages reverting to M2 macrophages. The transition from M1 to M2 macrophages indicates the switch from inflammation to proliferation phase of wound healing.[29] M2 macrophages are divided into M2a, M2b, M2c, and M2d subcategories by surface markers, with different secreted cytokines and biological functions. In particular, M2d macrophages release interleukin (IL)-10 and vascular endothelial growth factors (VEGFs), which may link the immunomodulatory function and angiogenesis during wound healing.[30–38] Macrophages also regulate neurogenesis after peripheral nerve injury, and M1 macrophages polarize towards M2 phenotype mediated by chemokine (C-C motif) ligand 2 (CCL2) and IL-10 in the milieus, whereas M2 macrophages release VEGF-A, promoting the formation of blood vessels to enable Schwann cells to migrate along the blood vessels and guiding the axonal regeneration.[39] Hence, angiogenesis and neurogenesis both mutually contribute to the resolution of inflammation and initiation of healing.[40] Macrophages may influence wound healing through the production of proteases which influence extracellular matrices (ECM) remodelling, and in the early and later phases of wound healing, M1 and M2 macrophages play different roles in regulating angiogenesis, neurogenesis, and ECM synthesis.[41] Wound closure progress and blood flow change have been significantly promoted in the TTT group on days 12 and 15, suggesting that TTT mainly promotes the proliferation phase of wound healing.

Recently, researchers discovered a microvascular network crossing the entire cortical bone between bone marrow cavities and bone surfaces in mice and human, referred to as trans-cortical vessels (TCVs).[42] Another previous study found that leucocytes travel against blood flow in TCVs, indicating that the TCV system may also be involved in modulating inflammation.[43] Therefore, TTT surgery may also stimulate the TCV system in the cortices, to promote angiogenesis as well as immunomodulatory effects.

In addition to its local stimulation, the TTT procedure may also induce systemic responses. Li et al[14] reported one case who had a recurrent and slow healing diabetic ulcer in the left tibia, and the TTT surgery was performed on the contralateral right tibia, while the size of the ulcer in the left tibia also reduced significantly. Systemic responses of DH include the mobilization of bone marrow-derived EPCs or mesenchymal stem cells (MSCs) and changes of circulating cytokines, triggered by mechanotransduction.[44] The common mechanotransduction signalling molecules include the yes-associated protein (YAP), tafazzin (TAZ), and extracellular signal-related kinase 1/2 (ERK1/2), which are involved in mechanical stress-induced osteogenic differentiation of MSCs or endothelial cell vascularization.[45,46] Positive systemic responses following TTT surgery would be appealing, as the TTT procedure is usually less invasive than the DH procedure.

Despite these encouraging findings, limitations remain in the current study. First, it only revealed the positive effects of TTT treatment on wound healing at an early stage, and its effects on the later stage of wound remodelling were not studied. It has been reported that TTT surgery could lead to scarless tissue formation with improved tactile sensation, suggesting that TTT might affect neurogenesis in wound healing.[21] As a result, the TTT effect on neurogenesis in the wound needs further investigation. Second, we only used healthy SD rats in the current study, so although the promoting effects of TTT surgery on wound healing in the normal rats were well established, we shall evaluate the effects of TTT surgery on diabetic rat wound healing in future studies. We hope that the current TTT model will enable us to study deeper biological mechanisms of TTT surgery, and improve its clinical applications to benefit patients in need.

Supplementary material

Figures comparing the mean wound healing rate with or without tibial cortex transverse transport treatment in the pilot study, and illustrating the power calculation performed based on the pilot study data.

References

1. **Kinlay S**. Management of Critical Limb Ischemia. *Circ Cardiovasc Interv.* 2016;9(2):e001946.

2. **Martins-Mendes D**, **Monteiro-Soares M**, **Boyko EJ**, **et al**. The independent contribution of diabetic foot ulcer on lower extremity amputation and mortality risk. *J Diabetes Complications.* 2014;28(5):632–638.

3. **Minematsu K**, **Tsuchiya H**, **Taki J**, **Tomita K**. Blood flow measurement during distraction osteogenesis. *Clin Orthop Relat Res.* 1998;347:229–235.

4. **Gubin AV**, **Borzunov DY**, **Marchenkova LO**, **Malkova TA**, **Smirnova IL**. Contribution of G.A. Ilizarov to bone reconstruction: historical achievements and state of the art. *Strategies Trauma Limb Reconstr*. 2016;11(3):145–152.

5. **Aston JW**, **Williams SA**, **Allard RN**, **Sawamura S**, **Carollo JJ**. A new canine cruciate ligament formed through distraction histogenesis. Report of a pilot study. *Clin Orthop Relat Res*. 1992;280:30–36.

6. **Ilizarov GA**. The tension-stress effect on the genesis and growth of tissues. Part I. The influence of stability of fixation and soft-tissue preservation. *Clin Orthop Relat Res*. 1989;238:249–281.

7. **Ilizarov GA**. Clinical application of the tension-stress effect for limb lengthening. *Clin Orthop Relat Res*. 1990;250:8–26.

8. **Gourdine-Shaw MC**, **Lamm BM**, **Paley D**, **Herzenberg JE**. Distraction osteogenesis for complex foot deformities: U-osteotomy with external fixation. *J Bone Joint Surg Am*. 2012;94-A(15):1420–1427.

9. **Stewart S**, **Darwood A**, **Masouros S**, **Higgins C**, **Ramasamy A**. Mechanotransduction in osteogenesis. *Bone Joint Res*. 2020;9(1):1–14.

10. **Salih S**, **Mills E**, **McGregor-Riley J**, **Dennison M**, **Royston S**. Transverse debridement and acute shortening followed by distraction histogenesis in the treatment of open tibial fractures with bone and soft tissue loss. *Strategies Trauma Limb Reconstr*. 2018;13(3):129–135.

11. **Kong L**, **Li HA**, **Kang Q**, **Li G**. An update to the advances in understanding distraction histogenesis: from biological mechanisms to novel clinical applications. *J Orthop Translat*. 2020;25:3–10.

12. **Qu L**, **Wang A**, **Tang F**. The therapy of transverse tibial bone transport and vessel regeneration operation on thromboangitis obliterans. *Zhonghua Yi Xue Za Zhi*. 2001;81(10):622–624.

13. **Hua Q**, **Zhang Y**, **Wan C**, **et al**. Chinese Association of Orthopaedic Surgeons (CAOS) clinical guideline for the treatment of diabetic foot ulcers using tibial cortex transverse transport technique (version 2020). *J Orthop Translat*. 2020;25:11–16.

14. **Li G**, **Ling SKK**, **Li HA**, **Zhang Y**, **Hu J**. How to perform minimally invasive tibial cortex transverse transport surgery. *J Orthop Translat*. 2020;25:28–32.

15. **No authors listed**. BFIX. Aike Shanghai Medical Instrument Co. Ltd. 2022. http://www.bfix.cn/ (date last accessed 18 February 2022).

16. **Wang C**, **Liang C**, **Wang R**, **et al**. The fabrication of a highly efficient self-healing hydrogel from natural biopolymers loaded with exosomes for the synergistic promotion of severe wound healing. *Biomater Sci*. 2019;8(1):313–324.

17. **Li Y**, **Pan Q**, **Zhang N**, **et al**. A novel pulsed electromagnetic field promotes distraction osteogenesis via enhancing osteogenesis and angiogenesis in a rat model. *J Orthop Translat*. 2020;25:87–95.

18. **Wolf G**. New insights into the pathophysiology of diabetic nephropathy: from haemodynamics to molecular pathology. *Eur J Clin Invest*. 2004;34(12):785–796.

19. **Clayton W**, **Elasy TA**. A review of the pathophysiology, classification, and treatment of foot ulcers in diabetic patients. *Clin Diabetes*. 2009;27(2):52–58.

20. **Paraskevas KI**, **Baker DM**, **Pompella A**, **Mikhailidis DP**. Does diabetes mellitus play a role in restenosis and patency rates following lower extremity peripheral arterial revascularization? A critical overview. *Ann Vasc Surg*. 2008;22(3):481–491.

21. **Chen Y**, **Kuang X**, **Zhou J**, **et al**. Proximal tibial cortex transverse distraction facilitating healing and limb salvage in severe and recalcitrant diabetic foot ulcers. *Clin Orthop Relat Res*. 2020;478(4):836–851.

22. **Eming SA**, **Brachvogel B**, **Odorisio T**, **Koch M**. Regulation of angiogenesis: wound healing as a model. *Prog Histochem Cytochem*. 2007;42(3):115–170.

23. **Chang CJ**, **Jou IM**, **Wu TT**, **Su FC**, **Tai TW**. Cigarette smoke inhalation impairs angiogenesis in early bone healing processes and delays fracture union. *Bone Joint Res*. 2020;9(3):99–107.

24. **DiPietro LA**. Angiogenesis and wound repair: when enough is enough. *J Leukoc Biol*. 2016;100(5):979–984.

25. **Gu Q**, **Yang H**, **Shi Q**. Macrophages and bone inflammation. *J Orthop Translat*. 2017;10:86–93.

26. **Chow SK**, **Chim YN**, **Wang JY**, **Wong RM**, **Choy VM**, **Cheung WH**. Inflammatory response in postmenopausal osteoporotic fracture healing. *Bone Joint Res*. 2020;9(7):368–385.

27. **Daley JM**, **Brancato SK**, **Thomay AA**, **Reichner JS**, **Albina JE**. The phenotype of murine wound macrophages. *J Leukoc Biol*. 2010;87(1):59–67.

28. **Lucas T**, **Waisman A**, **Ranjan R**, **et al**. Differential roles of macrophages in diverse phases of skin repair. *J Immunol*. 2010;184(7):3964–3977.

29. **Mosser DM**, **Edwards JP**. Exploring the full spectrum of macrophage activation. *Nat Rev Immunol*. 2008;8(12):958–969.

30. **Yao Y**, **Xu XH**, **Jin L**. Macrophage Polarization in Physiological and Pathological Pregnancy. *Front Immunol*. 2019;10:792.

31. **Zhou D**, **Huang C**, **Lin Z**, **et al**. Macrophage polarization and function with emphasis on the evolving roles of coordinated regulation of cellular signaling pathways. *Cell Signal*. 2014;26(2):192–197.

32. **Wang N**, **Liang H**, **Zen K**. Molecular mechanisms that influence the macrophage m1-m2 polarization balance. *Front Immunol*. 2014;5:614.

33. **Mills CD**. M1 and M2 macrophages: oracles of health and disease. *Crit Rev Immunol*. 2012;32(6):463–488.

34. **Mantovani A**, **Sozzani S**, **Locati M**, **Allavena P**, **Sica A**. Macrophage polarization: tumor-associated macrophages as a paradigm for polarized M2 mononuclear phagocytes. *Trends Immunol*. 2002;23(11):549–555.

35. **Wang LX**, **Zhang SX**, **Wu HJ**, **Rong XL**, **Guo J**. M2b macrophage polarization and its roles in diseases. *J Leukoc Biol*. 2019;106(2):345–358.

36. **Lee SH**, **Charmoy M**, **Romano A**, **et al**. Mannose receptor high, M2 dermal macrophages mediate nonhealing *Leishmania major* infection in a Th1 immune environment. *J Exp Med*. 2018;215(1):357–375.

37. **Farrow AL**, **Rana T**, **Mittal MK**, **Misra S**, **Chaudhuri G**. Leishmania-induced repression of selected non-coding RNA genes containing B-box element at their promoters in alternatively polarized M2 macrophages. *Mol Cell Biochem*. 2011;350(1–2):47–57.

38. **Chistiakov DA**, **Bobryshev YV**, **Nikiforov NG**, **Elizova NV**, **Sobenin IA**, **Orekhov AN**. Macrophage phenotypic plasticity in atherosclerosis: the associated features and the peculiarities of the expression of inflammatory genes. *Int J Cardiol*. 2015;184:436–445.

39. **Wu J**, **Xie H**, **Yao S**, **Liang Y**. Macrophage and nerve interaction in endometriosis. *J Neuroinflammation*. 2017;14(1):53.

40. **Porcheray F**, **Viaud S**, **Rimaniol AC**, **et al**. Macrophage activation switching: an asset for the resolution of inflammation. *Clin Exp Immunol*. 2005;142(3):481–489.

41. **Rappolee DA**, **Mark D**, **Banda MJ**, **Werb Z**. Wound macrophages express TGF-alpha and other growth factors in vivo: analysis by mRNA phenotyping. *Science*. 1988;241(4866):708–712.

42. **Grüneboom A**, **Hawwari I**, **Weidner D**, **et al**. A network of trans-cortical capillaries as mainstay for blood circulation in long bones. *Nat Metab*. 2019;1(2):236–250.

43. **Herisson F**, **Frodermann V**, **Courties G**, **et al**. Direct vascular channels connect skull bone marrow and the brain surface enabling myeloid cell migration. *Nat Neurosci*. 2018;21(9):1209–1217.

44. **Jin L**, **Deng Z**, **Zhang J**, **et al**. Mesenchymal stem cells promote type 2 macrophage polarization to ameliorate the myocardial injury caused by diabetic cardiomyopathy. *J Transl Med*. 2019;17(1):251.

45. **Rhee ST**, **El-Bassiony L**, **Buchman SR**. Extracellular signal-related kinase and bone morphogenetic protein expression during distraction osteogenesis of the mandible: in vivo evidence of a mechanotransduction mechanism for differentiation and osteogenesis by mesenchymal precursor cells. *Plast Reconstr Surg*. 2006;117(7):2243–2249.

46. **Dupont S**, **Morsut L**, **Aragona M**, **et al**. Role of YAP/TAZ in mechanotransduction. *Nature*. 2011;474(7350):179–183.

Author information:

- Y. Yang, MD, PhD student
- Y. Li, MD, PhD, Doctor
- S. Bai, MD, PhD student
- H. Wang, MD, PhD, Doctor
- K-K. Ling, MD, Doctor
- G. Li, MD, DPhil (Oxon), Doctor
  Department of Orthopaedics & Traumatology, Stem Cells and Regenerative Medicine Laboratory, Li Ka Shing Institute of Health Sciences, The Chinese University of Hong Kong, Prince of Wales Hospital, Hong Kong, China.
- Q. Pan, MD, PhD, Doctor, Department of Pediatric Orthopaedics, South China Hospital, Health Science Center, Shenzhen University, Shenzhen, China.
- X. Pan, MD, PhD, Doctor, Department of Orthopaedics and Traumatology, The Second Affiliated Hospital of Shenzhen University (Shenzhen Bao'an People's Hospital), Shenzhen, China.

ICMJE COI statement:
■ The authors have no conflicts of interest to disclose in relation to this article.

Data sharing:
■ All requests for raw and analyzed data and materials are promptly reviewed by the Technology Licensing Office of The Chinese University of Hong Kong to verify whether the request is subject to any intellectual property or confidentiality obligations. Any data and materials that can be shared will be released via a Material Transfer Agreement.

Ethical review statement:
■ All experiments were approved by the Animal Research Ethics Committee of The Chinese University of Hong Kong (AEEC no. 20-095-ECS).

Open access funding
■ The authors report that they received open access funding for their manuscript from the University Grants Committee, Research Grants Council of the Hong Kong Special Administrative Region, China (T13-402/17-N).